Semana Nacional de Engenharia Nuclear e da Energia e Ciências das Radiações - VII SENCIR
Belo Horizonte, 12 a 14 de novembro de 2024

Id.: EN-22

ADVANCED CANDU REACTOR PRESSURE TUBE CFD SIMULATION: POROUS MEDIA MODELING AND EVALUATION OF DIFFERENT VOLUMETRIC POWER GENERATION PROFILES

A.G. Moreira[1], C.S.L. de Carvalho[1], I.M. Gomide[1], I.K. Umezu[1], A.L. Costa[1,2]

[1] UFMG - Universidade Federal de Minas Gerais, DEN - Departamento de Engenharia Nuclear, Brazil
[2] INCT - CNPq National Institute of Science and Technology – Modular and Innovative Nuclear Reactors, Brazil
augustoguimaraesmoreira8@gmail.com

Keywords: CFD, Porous Media, CANDU, Thermal-Hydraulics

ABSTRACT

As the world´s clean energy demands expand, nuclear power is expected to follow and increase its share in the global power generation. In this context, theoretical studies in reactor safety and thermal-hydraulics are essential for ensuring this expansion. This study focuses in comparing computational cost of axial heat generation functions for the Advanced Candu Reactor (ACR) pressure tube using a porous media approach. The porous media coefficients were calculated based on available geometry and pressure drop data for the ACR assemblies, and several functions were evaluated in order to verify their applicability in this simplified computational model. The results are then compared with the available data.

1. INTRODUCTION

Computational Fluid Dynamics (CFD) has become an important tool for solving three-dimensional flow problems related to nuclear power plant safety and advanced reactor analyses. In recent years, the Working Group on the Analysis and Management of Accidents (WGAMA) of the Nuclear Energy Agency (NEA) has emphasized the use of CFD in nuclear safety research [1]. In this sense, the aim of this work is to contribute to research into the application of CFD for advanced nuclear reactors such as the ACR-700.

The ACR-700 reactor, developed by Atomic Energy of Canada Limited (AECL) as an evolution of the CANDU line, aimed to improve the efficiency and economic competitiveness of heavy water-moderated nuclear reactors. The ACR-700 uses slightly enriched uranium as fuel, with pressurized light water as coolant and heavy water as the moderator. The reactor core features a central structure called the calandria, which contains 284 pressure tubes, each with 12 CANFLEX fuel bundles arranged in line, as it is shown in Fig. 1.

Given the simple geometry and extensive available technical documentation, this reactor was selected as the basis of this research. This work aims to simulate, using CFD on ANSYS Fluent R19.3, different energy generation functions — constant, cosine, parabolic, polyfit — applied in the most heated pressure tube of ACR-700, to compare them and analyze their respective computational costs. The polyfit function is a six degree polynomial fit of an original design function. Simulations were conducted in steady state operation.

The geometry of the pressure tube was modeled in SpaceClaim, and the fuel assemblies were discretized as one porous region, determined based on the initial design pressure drop data. The model

accounts for the constant properties of the coolant and varying power distributions were applied to represent the non-uniform heat generation within the fuel assemblies.

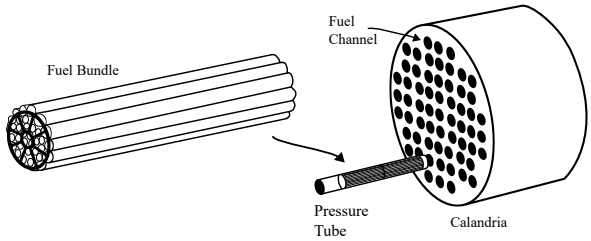

Fig. 1. Calandria and Pressure Tube visual representation

A review of the literature reveals that studies have modeled CANDU 6 reactor components using different approaches, but not ACR-700. Study [2] analyzes flow in specific parts of a CANDU 6 pressure tube, like junctions and fuel bundle spacers, while this work addresses the entire tube and assembly of ACR-700. Study [3] focuses on coolant flow and pressure loss but does not use the porous media model, which is applied here to simplify the geometry. Research [4] also uses porous media approach but for simulating all pressure tubes, whereas this study examines one ACR pressure tube and compares the computational cost of different power profiles.

2. METHODOLOGY

2.1. Model Description and Assumptions

The model consists of a cylindrical geometry representing a simplified reactor pressure tube. It has an inlet at one of the extremities of the tube and an outlet at the other edge, with the fluid flow in the positive z-direction. The model is shown in Fig. 2 with geometry data presented in Tab. 1.
The region of the tube where the fuel bundles are stacked is defined as the active area, hence, it is where porous media and volumetric power functions are applied. The cross-sectional area of the bundles was used to calculate the porosity of the tube as, in this geometry, to the ratio of the area is proportional to the ratio of the volume.

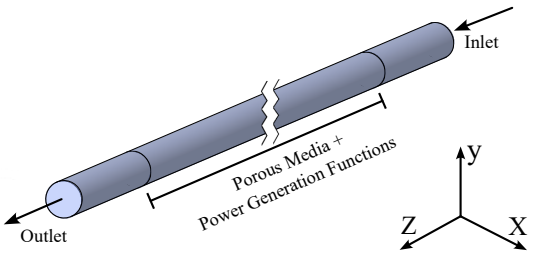

Fig. 2. Domain sketch.

Tab. 1. Main geometry parameters.

Domain Geometry	**Value**	**Units**
Radius	51.69	$[mm]$
Total length	7.47	$[m]$
Active length (L)	6.27	$[m]$
Cross-section Area (A)	8393.50	$[mm^2]$
Bundle-section Area (A1)	4780.60	$[mm^2]$
Porosity $(1 - A1/A)$	0.4304	–

2.1.1. Boundary Conditions (BCs)

For inlet, 13 MPa pressure and 551 K temperature were set; for outlet, Mass Flow Rate of $\dot{m} = 26\ kg/m^3$ [5]. Walls were defined as zero-shear, as the porous model covers friction and energy losses, removing the need to account for velocity gradients. Walls were also treated as adiabatic, as the gas-filled gap between the pressure and calandria tubes limits heat conduction. [5].

2.2. Fluid Properties

To determine the thermophysical properties of the coolant, the properties values at the inlet, 551.65 K and 13 MPa, and at the outlet, 598.15 K and 12.2 MPa [5], were calculated in [6] and averaged. The calculated properties are presented in Tab. 2.

Tab. 2. Employed thermal-physical properties of light water.

Property	**Properties Values**	**Units**
Density (ρ)	709.105	$[kg/m^3]$
Thermal Conductivity (k)	0.5517	$[W/m\ K]$
Dynamic Viscosity (μ)	8.6411×10^{-5}	$[Pa\ s]$
Specific Heat (C_p)	5955.6	$[J/kg\ K]$

2.3. Mesh Size Definition

A primary objective of this study is to compare computational time between the simulations. Dealing with CFD, a less refined mesh implies in reduced simulation time, since fewer cells mean the solver has to process less data, perform fewer calculations, and solve the governing equations over a smaller number of points; making the comparison more difficult and susceptible to errors. Considering this, a mesh analysis is not performed in this study to select an optimal mesh size; instead, a refined mesh was directly chosen. Furthermore, since this is a comparative study, the mesh does not have a critical role as long as it is sufficiently fine to accurately capture the fluid behavior under the different power profiles. Chosen refined mesh specificities, along with a visual representation of the volume mesh around the outlet region, are presented in the following Tab. 3 and Fig. 3.

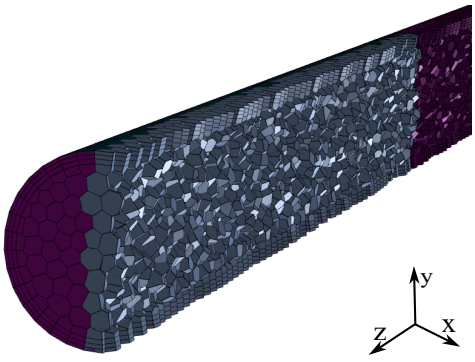

Fig. 3. Volume mesh detail around the outlet region.

Tab. 3. Mesh Parameters

Mesh Aspects	**Values**
Surface Mesh (min./max.) $[mm]$	5/10
Maximum Cell Length $[mm]$	10
Average Aspect Ratio	3.727
Maximum Aspect Ratio	7.245
Number of Volume Cells	174 460
Number of Inflation Layer	3
Minimum Orthogonal Quality	0.609
Average Orthogonal Quality	0.975

2.4. Pressure Drop

To model the pressure drop in the pressure tube, a porous medium approach was used. The porosity was calculated as 0.4304. The pressure drop was modeled using the calculated C_2 values, with a feedback loop in which the simulated velocity was used to iteratively refine the C_2 values. In the "z" direction, the value of C_2 was determined by Eq. 2.1.

$$C_2 = 2\frac{\Delta P}{\rho v^2 L} \tag{2.1}$$

The total pressure drop was set as $\Delta P = 800\,\text{k Pa}$, and the flow velocity was $v = 4.4\,\text{m/s}$ [5]. It result in $C_2 = 18.5882\,\text{m}^{-1}$. For the other directions, the coefficient was multiplied by 1000 to reduce cross-flow.

2.5. Thermal Power Axial Distribution Functions

The power density distribution in the pressure tube was modeled using different mathematical functions: constant, cosine, parabolic and polyfit. Each different profile influences the temperature distribution and, consequently, the thermal performance of the coolant. These functions are presented in Tab. 4.

Tab. 4. Volumetric Power Generation Functions.

Shape	**Function** $[\times 10^8\ W/m^3]$
Constant	$q'''_{con}(z) = 1.3871$
Cosine	$q'''_{cos}(z) = 2.0847 \cdot \cos\left(\pi \frac{(z-3.135)}{6.57}\right)$
Parabolic	$q'''_{par(z)} = 1.9918 \cdot (1 - 0.0927 \cdot z^2 + 0.581 \cdot z - 0.9108)$
Polyfit	$q'''_{fit}(z) = (10.329 + 884.98 \cdot z - 91.034 \cdot z^2 - 180.53 \cdot z^3$ $+78.358 \cdot z^4 - 12.329 \cdot z^5 + 0.6736 \cdot z^6) \cdot 19001.4 \cdot 11.732$

The total thermal power, $P_{\text{total}} = 7.3\,\text{MW}$, [5], is distributed across the active region of the pressure tube, which was defined as $V = A \cdot L$. Dividing P_{total} by V, the value of $1.3871 \times 10^8\ W/m^3$ is obtained. This value equals to the average volumetric power of the pressure tube and to the constant power density function, present in Tab. 4.
Each function was adjusted to produce the same total power of $1.3871 \times 10^8\ W/m^3$. For this, they were integrated over the length from $0\ m$ to L, divided by L and equalized to the constant function value. Their peak values were also normalized by factors designed for consistency.
The cosine and parabolic functions were also regulated to gradually approach to $0\ W/m^3$ at a small distance after active length extremities, since the power at these points is not exactly zero. This was achieved by adding $0.15\ m$ to each edge, resulting in an estimated extrapolated length of $L_e = L + 0.3\ m$. Polyfit, in other hand, was specifically derived from bundle-power profile data [5]. Its coefficients were chosen to reflect the power distribution.

Figure 4 illustrates these different volumetric power functions applied to the coolant.

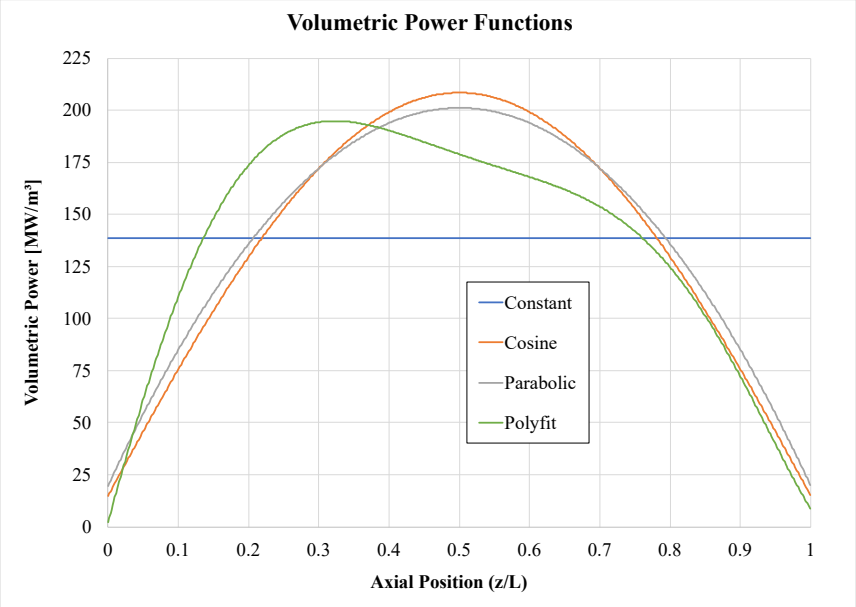

Fig. 4. Applied volumetric power functions.

Constant function maintains a linear power distribution along the axial position, while cosine and parabolic functions exhibits a peak at the center of the pressure tube with a symmetric distribution. Polyfit function have a left-displaced peak.

2.6. Computational Methods

Fluent's Pressure-velocity Coupled Solver was chosen, with the turbulence model being the $k-\omega$ SST. Relaxation factors were set to default: 0.5 in pressure and momentum; 0.75 in turbulent kinetic energy, Specific Dissipation Rate and Energy; 1 in Density, Turbulent Viscosity and Body Forces. The solution initialization method was set as Standard due to the presence of a porous region, and the convergence criterion was defined as 10^{-6} for all the scaled residuals [7]. The continuity, momentum, and energy equations solved in ANSYS Fluent are not presented in this brief paper but can be easily found in the literature [8].

2.6.1. Computational Comparison

To obtain the reports related to computational costs, used to compare the function in results section, a mean of 5 simulation reports on data transfer and time was taken for each of the 4 functions used in the study. This methodology was employed to minimize internal variances that could affect the results obtained. Such variances can include fluctuations in computational load due to varying levels of system activity, differences in initialization conditions, and potential numerical instabilities that might arise during different simulation runs. By averaging over multiple simulations, the aim is to reduce the impact of these factors and obtain a more stable and representative measure of computational cost.

3. RESULTS

Figure 5 depicts both the pressure drop and the coolant velocity as functions of the axial position. The pressure curve starts high and decreases steadily as the coolant moves through the tube. The obtained ΔP matches the reference data of $800\ kPa$ [5], which confirms that the porous media model used in the simulation is appropriate. Regarding coolant velocity, the profile remains constant for the majority of the axial length. However, near the end of the pressure tube, the velocity increase is a numerical anomaly and is negligible, with an increase of approximately 1%. A comparative analysis of the coolants temperature profiles resulting from each applied volumetric power function is presented in Fig. 6.

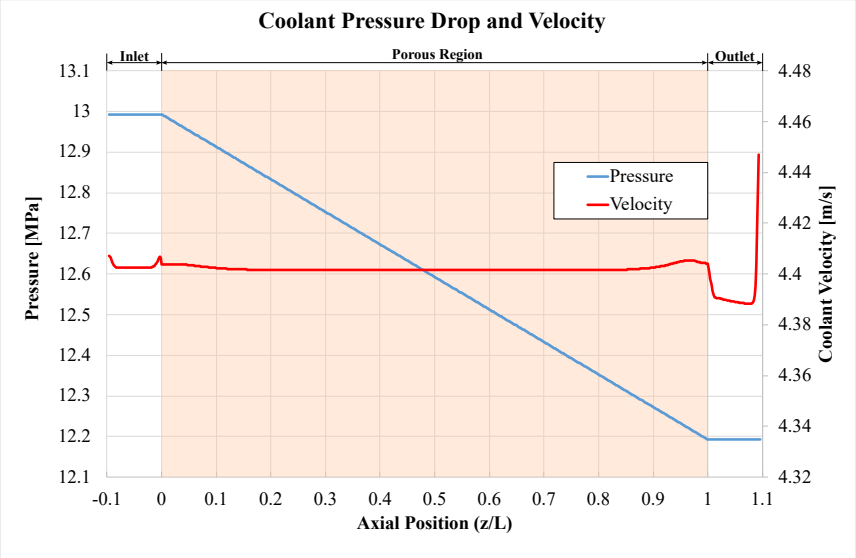

Fig. 5. Pressure drop and collant velocity as function of the axial position.

Regarding the constant function, the temperature increases linearly along the axial position, reflecting the uniform power distribution. Since the power and the fluid properties are constant, the temperature gradient is linear. At the cosine function, the temperature profile shows a moderate rise at the beginning and a steeper increase towards the middle, corresponding to the peak in power distribution in sinusoidal shape. After the peak, the temperature rise slows down. In parabolic function, the temperature rises similar to the cosine function, but more sharply in the middle of the tube. Polyfit heats up earlier compared to the other profiles due to the shape of the function, which increases more steeply at the beginning. After that, it behaves similarly to the other functions, stabilizing near the end.

The calculated temperature difference ΔT for each function is compared with the reference value of $46.5\ K$ [5] in Tab. 5. The error is determined by calculating the percentage difference between the reference and calculated values.

The ΔT values align with experimental data, and the comparison reveals that both polyfit and cosine functions provides the closest match to the reference, with the smallest difference. Additionally, the boundary conditions applied are suitable and match the expected values, validating the accuracy of the simulation setup.

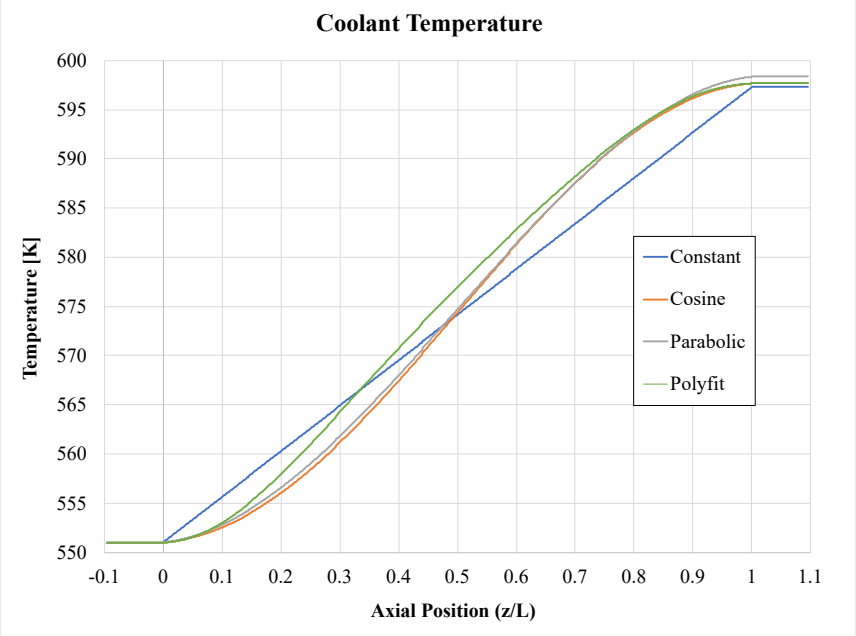

Fig. 6. Temperature comparison between functions.

Tab. 5. Values of ΔT and Error for different functions

Function	$\boldsymbol{\Delta T}$ $\boldsymbol{[K]}$	**Error** [%]
Reference [5]	46.50	–
Constant	46.29	0.5
Cosine	46.66	0.4
Parabolic	47.34	1.9
Polyfit	46.66	0.4

3.1. Computational Costs

In Table 6, the computational costs are presented in terms of data transfer per iteration (MB) and average wall-clock time per iteration (s). This data was directly extracted from ANSYS Fluent through the Time Usage report after the simulations were completed.
Table 6 indicates that the maximum difference in the provided data ($max-min$) is 16 bytes in terms of data transfer and 0.04 seconds in terms of time. These differences are minimal, what can be explained by analyzing the simulation scaled residuals, which show that the energy equation converges before the end of the simulation (in polyfit function, which has the highest cost in terms of data transfer, convergence occurs at iteration 107 out of 210). It implies, therefore, the total simulation time is not primarily determined by the energy equation, meaning its impact on computational cost is nearly negligible. Since there is no significant cost dependency on the chosen function, preference should be given to the one that best describes the system.

Tab. 6. Comparison of functions computational cost.

Function	**Data Transfer** (MB)	**Time** (s)
Constant	20.659	1.25
Cosine	20.667	1.29
Parabolic	20.662	1.25
Polyfit	20.675	1.23

4. CONCLUSIONS

The results of this study show that the porous media model is appropriate for simulating the ACR-700 pressure tube. The different power functions produced similar fluid temperature changes, with the smallest variations found in the constant, cosine, and polyfit functions. However, since the constant function is based on an average value, it does not accurately represent the shape of the volumetric power distribution. So, only cosine and the polyfit functions are better suited for simulation. In this case, computational cost differences are minimal and independent of energy, so they should not be a factor in choosing the volumetric power distribution function. The choice should depend on the goals of the user, whether ease of implementation or the best match to the expected profile.

ACKNOWLEDGEMENTS

The authors are thankful to the following Institutions: **CAPES** (*Coordenação de Aperfeiçoamento de Pessoal de Nível Superior*), **FAPEMIG** (*Fundação de Amparo à Pesquisa do Estado de Minas Gerais*), and **CNPq** (*Conselho Nacional de Desenvolvimento Científico e Tecnológico*).

REFERENCES

[1] N. E. Agency, "Requirements for cfd-grade experiments for nuclear reactor thermal hydraulics", Nuclear Energy Agency, OECD, Tech. Rep. NEA/CSNI/R(2020)3, Feb. 2022. [Online]. Available: https://www.oecd-nea.org.

[2] A. CATANA, I. PRISECARU, D. DUPLEAC, N.DANILA, *Cfd thermal-hydraulic analysis of a candu fuel channel*, Accessed: 2024-09-05, 2009. [Online]. Available: https://inis.iaea.org/collection/NCLCollectionStore/_Public/51/079/51079271.pdf.

[3] V. Diaconu and M. Pavelescu, *Cfd methods for thermal-hydraulic analysis of pressure tube nuclear reactors*, Accessed: 2024-09-05, 2011. [Online]. Available: http://www.jnrd-nuclear.ro/images/JNRD/No.1/JNRD_No1_paper07.pdf.

[4] G. H. Xu, Y. Qiu, and L. L. Wang, *Development for predicting the moderator temperature of candu-6 using a porous media approach*, Accessed: 2024-09-05, 2012. [Online]. Available: https://asmedigitalcollection.asme.org/ICONE/proceedings-abstract/ICONE20-POWER2012/265/293850.

[5] L. AECL, "Acr-700 technical description", Atomic Energy of Canada Limited, Technical Report ML032030391, 2003. [Online]. Available: https://www.nrc.gov/docs/ML0320/ML032030391.pdf.

[6] NIST Chemistry WebBook, *Nist chemistry webbook - fluid properties*, https://webbook.nist.gov/chemistry/fluid/, Accessed: 2024-09-12, 2024.

[7] I. ANSYS, *ANSYS Fluent User's Guide*. ANSYS, Inc., 2019.

[8] I. ANSYS, *User's guide: Ansys fluent*, Accessed: 2024-10-18, 2024. [Online]. Available: https://www.afs.enea.it/project/neptunius/docs/fluent/html/th/node322.htm.